universität wien

MASTERARBEIT / MASTER'S THESIS

Titel der Masterarbeit / Title of the Master's Thesis

„Microbial Degradation of Gelatinous Zooplankton Detritus"

verfasst von / submitted by

Jennifer Hennenfeind, BSc

angestrebter akademischer Grad / in partial fulfilment of the requirements for the degree of

Master of Science (MSc)

Wien, 2021 / Vienna, 2021

Studienkennzahl lt. Studienblatt / degree programme code as it appears on the student record sheet:	UA 066 833
Studienrichtung lt. Studienblatt / degree programme as it appears on the student record sheet:	Masterstudium Ecology and Ecosystems
Betreut von / Supervisor:	Univ.-Prof. Dr. Gerhard J. Herndl

ABSTRACT: In the last decades, the *Ctenophora Mnemiopsis leidyi* has invaded many marine ecosystems often causing drastic changes in pelagic community structures. As bloom forming gelatinous zooplankton, the ctenophore can reach high abundances and potentially contribute substantially to dissolved organic matter as well as inorganic nutrient pools via excretion and mucus production. The decay of *M. leidyi* carcasses might provide an organic-rich substrate to heterotrophic microbes in the ambient water. In this thesis, the microbial growth parameters were estimated and, dissolved organic carbon concentrations were measured to follow microbial dynamics after the collapse of ctenophore blooms and its implications on the ecology of coastal waters. We show that a decay of a typical ctenophore bloom, when approximately 100 mg of ctenophore detrital organic matter (cteno-OM) per liter becomes available, enriches the system with ~21 µM DOC (or 0.07±0.01 µmol per mg of cteno-OM) and triggers rapid microbial growth (μ = ~1.8 d^{-1}). Carbon derived from cteno-OM fuels microbial respiration rather than biomass production (bacterial growth efficiency ~22%). *Pseudoalteromonas*, *Alteromonas* and *Vibrio* together represent up to ~37% of all respiring bacterial cells and up to ~69% of the biomass producing bacterial community. Tinta et al. (2020) studied the degradation of *Aurelia aurita* applying an identical experimental set up. Comparing our findings to the study of Tinta *et al*. (2020), indicates that different sources of gelatinous zooplankton organic matter provoke differences in microbial and environmental responses.

1. INTRODUCTION

Marine heterotrophic microorganisms dominate the processing and remineralization of the largest organic carbon storage in the biosphere – the oceanic pool of dissolved organic matter (DOM) amounting to 662 Pg (Hansell *et al.*, 2009). A mechanistic understanding of these processes and dynamics of microbial communities as well as the fluxes of carbon in the ocean is indispensable to predict the future development of marine ecosystems in the light of climate change (Hoegh-Guldberg *et al.*, 2014).

1.1. Dissolved Organic Matter in the Ocean

About half of the Earth's primary production is mediated by marine photoautotrophic microorganisms, collectively coined phytoplankton, through carbon sequestration from the atmosphere via photosynthesis (Field *et al.*, 1998). Phytoplankton are grazed upon by herbivorous zooplankton and thereby initiating the transfer of energy to higher trophic levels. As a result, DOM becomes available through various processes: (a) extracellular release (ER) by phytoplankton, (b) grazer-mediated release and excretion, (c) release via cell lysis (both viral and bacterial), (d) solubilization of detrital and sinking particles, and (e) release from prokaryotes (Carlson and Hansell, 2015). The complex array of biomolecules within the DOM pool serves as a substrate for metabolically diverse marine heterotrophic bacteria. The participation and structure of these microbial communities as well as their metabolism depend on the quality and quantity of the available organic matter (Azam and Malfatti, 2007).

1.2. Gelatinous Zooplankton Organic Matter (GZ-OM)

Bloom-forming GZ populations (herein referred to as scyphozoans, ctenophores and pelagic tunicates) are ubiquitous in the global oceans and capable of coping with a wide range of environmental conditions (Richardson *et al.*, 2009; Lucas *et al.*, 2014). Representative taxa inhabit estuarine, coastal, and open water ecosystems throughout the global oceans, while major GZ blooms have been reported especially in coastal areas (Condon *et al.*, 2013; Lucas *et al.*, 2014). The global GZ biomass in the epipelagic ocean amounts to ~510 Tg C, of which ~57% have been attributed to *Scyphozoa* (phylum Cnidaria) and ~40% to *Ctenophora* (Luo *et al.*, 2020). The biomass of GZ is characterized by large variations in space and time, a result of bloom events upon which populations reach high individual abundances within a short period

of time followed by mass mortality once conditions are less favorable (Pitt *et al.*, 2014). GZ blooms are triggered by favorable environmental conditions and can persist from weeks to months. Reasons determining the collapse of GZ blooms are still largely unknown (Tinta, Klun and Herndl, 2021). Contributing factors were reviewed by Pitt *et al*. (2014) and include food limitation, predation, parasitism and bacterial infections and loss of tentacles leading to starvation. Abiotic environmental parameter such as water temperature, (low) salinity, and ultraviolet radiation in shallow waters might be among the physical variables leading to a population collapse (Pitt *et al.*, 2014). Regardless of the reason, the collapse of GZ blooms can result in significant amounts of carbon, nitrogen and phosphorus within DOM pool becoming available to the pelagic community (Pitt, Welsh and Condon, 2009; Tinta, Klun and Herndl, 2021). Hence, GZ can have significant impacts on local DOM pools and biogeochemical cycles (Pitt, Welsh and Condon, 2009; Richardson *et al.*, 2009; Condon *et al.*, 2011; Lucas *et al.*, 2014; Lebrato *et al.*, 2019; Luo *et al.*, 2020; Wright *et al.*, 2020; Tinta, Klun and Herndl, 2021). Furthermore, the understanding of GZ boom and bust populations is crucial for several environments exhibiting longer and more frequent blooms than in the past decades, often leading to drastic socio-economic consequences (Richardson *et al.*, 2009; Purcell, 2011; Condon *et al.*, 2013). Due to their pronounced adaptive capability an increase in blooming events could be the result of predicted future ocean scenarios such as in a warmer, more acidic, and less oxygen containing ocean (Richardson *et al.*, 2009; Kogovšek, Bogunović and Malej, 2010; Purcell, 2011; Hoegh-Guldberg *et al*., 2014; Steinberg and Landry, 2017).

1.3. Microbial degradation of GZ-OM

Upon the collapse of blooming populations, dead GZ carcasses can be a) consumed and/or fragmented by scavengers, b) sink to the benthos as “jelly-falls” where they are available for benthic communities, c) degraded by planktonic communities and/or the detrital DOM is remineralized by planktonic microbial communities (Billett *et al.*, 2006; Lebrato *et al.*, 2012; Sweetman *et al.*, 2014; Dunlop, Jones and Sweetman, 2017; Luo *et al.*, 2020; Tinta *et al.*, 2020; Tinta, Klun and Herndl, 2021).

The biochemical composition of jellyfish and ctenophore OM (cteno-OM) is characterized by the lack of an exoskeleton, a high water content (~95%), a low C:N ratio (~4.5:1; Pitt, Welsh and Condon, 2009; Lucas *et al.*, 2011; Kogovšek *et al.*, 2014;

Molina-Ramírez *et al.*, 2015), a high protein content (72±14%) and a low lipid content (22±12%) (Pitt, Welsh and Condon, 2009), making it a particularly attractive source of easy degradable and fast accessible substrate for the heterotrophic bacterioplankton community. The DOM amounts captured within the GZ species *Aurelia aurita,* for example, can make up to one half of the entire organic matter biomass of an individual (Tinta *et al.*, 2020). Furthermore, several GZ taxa show a high bioavailability for degrading microbes in the ambient water (Pitt, Welsh and Condon, 2009; Tinta *et al.*, 2010, 2020; Blanchet *et al.*, 2015a). The common conclusion drawn from the available microbial GZ-OM degradation studies (Titelman *et al.*, 2006; Tinta *et al.*, 2010, 2012, 2016, 2020) is a rapid stimulation of bacteria with growth rates between 0.2–7 d^{-1} (Titelman *et al.*, 2006; Tinta *et al.*, 2010), exceeding commonly reported bacterial growth rates (0.1–1 d^{-1} Ducklow, 1999; Kirchman, 2016) for the ocean. Furthermore, characteristic shifts in the bacterial community have been reported when GZ-OM is abundant from *Alphaproteobacteria* to *Gammaproteobacteria*, representing between 40–90% of the GZ-OM degrading bacteria (Tinta *et al.*, 2012, 2016, 2020; Blanchet *et al.*, 2015a). So far, scientific research on GZ decay and degradation has mainly focused on *Scyphozoa* (Hansson, 1997; Titelman *et al.*, 2006; West, Welsh and Pitt, 2009; Chelsky, Pitt and Welsh, 2015; Sweetman *et al.*, 2016; Tinta, Klun and Herndl, 2021). To our knowledge, only one study has focused on targeting actively respiring and producing key players of bacteria during jellyfish-OM decomposition (Tinta *et al.*, 2020). As GZ are a functionally and morphologically diverse group of metazoans, further assessment of decomposition processes during the decay of non-*Scyphozoa* GZ species is required to understand the impact of decaying GZ blooms on the surrounding system.

Ctenophora, representing 40% of the GZ carbon stock (Luo *et al.*, 2020), share some common features with scyphozoans, such as a transparent gelatinous tissue, a simple body plan, high water content, comparable dry weight and similar elemental ratio as *Scyphozoa*. Nonetheless, crucial differences exist between the two taxa, namely the absence or presence of nematocysts as well as different life histories and reproduction strategies which could have important implications for interacting microbes (Tinta, Klun and Herndl, 2021). Additionally, *Ctenophora* are generally smaller and more fragile than *Syphozoa*. Thus far, there are no records of deposition of ctenophore carcasses at the seafloor (so called “jelly-falls”, Luo *et al.*, 2020). This might indicate that the degradation process exhibits different dynamics than that of scyphozoans.

In the framework of this thesis, we aim at elucidating the processes and key players during the degradation of the invasive ctenophore species *M. leidyi.*

1.4. Ctenophore Mnemiopsis leidyi

M. leidyi, originally native to the waters along the Atlantic coast of North and South America, has been invading new habitats since the early 1980s, when it was first observed in the Black Sea (Vinogradov *et al*., 1989). There, it contributed to the collapse of the entire Black Sea commercial fisheries and to the depletion of zooplankton stocks (Shiganova, 1998). It successfully spread further to many areas of the Eurasian seas (Costello *et al.*, 2012). In 2016, the first dense blooms in the northern Adriatic Sea were recorded from mid-August to November (Malej *et al.*, 2017). Large populations of *M. leidyi* are regularly observed between July and November, reaching populations densities of up to 300-500 individuals per m^2 (Pestorić *et al.*, 2021). The ctenophore has become an ecological model organism for biological invasions often leading to significant changes in food web structure and function (Tiselius and Møller, 2017; Jaspers *et al.*, 2018).

Since the chemical composition of ctenophores and scyphozoans is comparable (Anninsky *et al.*, 2005; McNamara, Lonsdale and Aller, 2013), cteno-OM available after blooms might have similar implications on the local systems as “true” jellyfish (Scyphomedusae) such as *A. aurita*. The capability of *M. leidyi* to stimulate bacterioplankton growth and to select for certain bacterial taxa in its vicinity has been shown (West *et al.*, 2009; Condon *et al.*, 2011; Dinasquet, Granhag and Riemann, 2012; Dinasquet *et al.*, 2013). However, the processes and key players of degrading ctenophore carcasses following the collapse of blooming events remain unknown.

1.5. Objective of the study

The main objective of this cteno-OM incubation experiment was to investigate the microbial processes during *M. leidyi* biomass decay. Therefore we conducted a cteno-OM incubation experiment, simulating conditions potentially experienced by the ambient microbial community of the Gulf of Trieste (northern Adriatic Sea) during a typical ctenophore bloom decay. In the enclosures we followed the response of the ambient microbial community to this type of organic matter by analyzing bacterial community growth rates, changes of community composition (via taxonomic profiling

of metagenomes), and the respiration and production of dominant bacterial populations. The measurements of abiotic parameters included inorganic nutrients, DOC, DON and dissolved amino acids. By assessing this large array of biological and chemical parameters we aimed at obtaining insight into the bacterial decomposition of ctenophore detritus. Targeting a part of this comprehensive project, this MSc. thesis addresses the following research questions: How are microbial growth parameters and DOC dynamics changing during the course of cteno-OM degradation? Does the incubation with detrital cteno-OM influence the respiring and/or producing ambient microbial community? Does cteno-OM incubation trigger the same microbial responses as detrital jelly-OM from *A. aurita*?

2. MATERIAL AND METHODS

2.1. Experimental Setup

The short-term cteno-OM degradation experiment was conducted at the University of Vienna in October 2019. The experiment was set up using six combusted 10 L borosilicate glass flasks filled with 9 L of 0.2 µm filtered aged seawater (ASW) and 1 L of 1.2 µm pre-filtered bacterial inoculum to reach a starting cell abundance of ~$1x10^5$ cells mL^{-1}. Three of the enclosures were enriched with 100 mg L^{-1} of *M. leidyi* powder, prepared as described below (thereafter, J1, J2, J3). Flasks without ctenophore amendment served as controls (C1, C2, C3). All glass bottles were incubated at *in situ* temperature in the dark from the beginning (14^{th} Oct 2019) to the end (21 Oct 2019) of the experiment. The entire glassware used for the experiment was pre-washed with 1% HCL and rinsed with Milli-Q water before combusting at 450°C for 4 h. All non-combustible labware was washed with 1% HCL, rinsed with Milli-Q water and dried before use.

2.2. Sampling of the media, microbial inoculum, and M. leidyi individuals

To obtain ASW, surface seawater from the Bay of Piran (Gulf of Trieste) was collected with Nalgene bottles in August 2019. The water was then aged at room temperature in the dark in the laboratory of the Microbial Oceanography Unit at the University of Vienna. Prior to the experiment, the ASW was twice filtered through 0.2 µm polycarbonate filters and 9 L were added to each of the six borosilicate glass flasks.

The seawater for the bacterial inoculum was sampled right before the start of the experiment, on 14th Oct 2019, using 5 L Niskin bottles connected to a carousel water sampler (SBE 32, Sea-Bird Electronics) in the Bay of Piran at the oceanographic buoy Vida (45°32.93′ N, 13° 33.03′ E) at 5 m depth. The seawater was then transferred to Nalgene bottles and transported to the laboratory in Vienna while being kept in the dark within 12 h after sampling. Before adding the bacterial inoculum to the 9 L of ASW, it was filtered through 1.2 µm polycarbonate filters using a 47 mm diameter glass filtration set to remove particles and organisms > 1.2 µm. Just prior to the beginning of the experiment, 1 L of the filtered bacterial inoculum was added to each of the nine bottles.

Twenty-one individuals of *M. leidyi* were sampled during their bloom from the surface waters in the Gulf of Trieste using a clean bucket rinsed with ambient seawater at the end of September 2019 (Supplement 1). Each individual was then immediately transferred into a sterile 50 mL Greiner tube which was stored in a cooling tank protected from light during transportation. In the laboratory of the National Institute of Biology (NIB) at Piran, the samples were stored at –20°C. To preserve its biochemical properties and to ensure homogeneity of the material as well as the reproducibility of the experiments, each individual ctenophore was first freeze-dried (at –45°C for 7 d, as described elsewhere (Kogovšek *et al.*, 2014) and finally grinded with a sterilized agate mortar and pestle. Then, the dry weight (DW) for each specimen was determined (

Supplement *1*) and the ctenophore powder stored in combusted glass vials at –20°C until used.

At the beginning of the experiment, 100 mg L^{-1} of ctenophore powder was added to the three of the glass enclosures (J1, J2, J3). This amount represents the abundance observed under bloom conditions by the ambient microbial community in the northern Adriatic Sea, corresponding to, on average, seven individuals per m^3 in the water column (Kogovšek and Malej, person. comm).

2.3. Subsampling of the experiment

Bottles were subsampled right after inoculation, and then after 4, 9, 17, 21, 58, 82 and 154 h (T0–T7). Samples for bacterial abundance (1.5 mL) and DOC (30 mL) were taken each sampling. Additional subsamples were taken from 1) the bacterial

inoculum, 2) from the late exponential phase (T4 = 21 h) and 3) from the senescent phase (T7 = 154 h) for DOC (2 x 30 mL), for sub-incubation with Redox Sensor Green (RSG; 3 x 5 mL), sub-incubation with homopropargylclycine (HPG, 3 x 5 mL). Subsamples were taken as technical replicates (2–3). Sub-incubations will be explained in Section 2.8 Respiration and production of specific bacterial populations. Including the additional subsamples taken, which are not discussed in the framework of this thesis, the volume taken from each individual bottle at each timepoint was < 250 mL. Thus, more than 2/3 of the initial volumes were still left in the bottles at the end of the experiment.

2.4. Estimating microbial cell abundance

Samples for microbial abundance were immediately fixed with formaldehyde (2% final concentration) and stored in 2 mL Cryo Tubes at –80°C until further analyzed. One of the three replicates was examined under the epifluorescence microscope after fixation with formaldehyde (2% final concentration to follow microbial growth during the experiment in near real-time. Therefore, 1 mL was filtered onto an 0.2 µm white polycarbonate filter (Millipore) with an 0.45 µm cellulose nitrate support filter (Millipore), which was then transferred onto a glass slide, stained with two drops of 4′,6-diamidine-2′-phenylindole dihydrochloride (DAPI) solution in Vectashield (2 µg mL^{-1} final concentration) and covered with a cover slide. This procedure was repeated for all three replicates at all timepoints of the experiment. Cell counts were done directly under the epifluorescence microscope (Zeiss Axio Imager M2 at 1,250 magnification and the DAPI filter set, Ex/Em = 358/461 nm). Cells in 20 randomly selected fields were counted manually. In each counting field between 20–200 cells were enumerated.

2.5. Dissolved organic carbon (DOC) measurements

The samples for DOC/TDN were filtered through combusted Whatman GF/F filters (~ 0.8 µm) using a glass filtration set (1M HCl, MilliQ pre-washed and combusted) during the experiment. Then the filtrate (approx. 30 mL) was collected into glass vials and acidified with 12 M HCL (~100 µL per ~ 20 mL of sample) to reach a final pH < 2. The glass vials were stored at 4°C until further analyzed at NIB in Piran. DOC analyses were performed with a high temperature catalytic method using Shimadzu TOC-L

analyzed (Hansell, Williams and Ward, 1993). The calibration for non-purgeable organic carbon (NPOC) was done with potassium phthalate. The results were validated with low carbon water and Deep-Sea Reference (DSR) water material for DOC (CRM Program, Hansell Lab). The precision of the method expressed as RSD % was < 2%. The filtration system and all other glass ware were acid-, Milli-Q-washed and combusted.

2.6. Calculating bacterial growth parameters

Bacterial growth parameters were calculated from bacterial cell counts (cell mL^{-1}) and DOC concentrations (µmol L^{-1}). Assuming that the bacterial metabolism was fueled by DOC only, the decrease in DOC represents the heterotrophic bacterial carbon demand (BCD). The DOC taken up by the bacterial community is used for the synthesis of new bacterial biomass and for respiration. From the increase of bacterial biomass (BB, assuming a C-content of 20 fg C $cell^{-1}$ (Lee and Fuhrman, 1987) during the exponential growth phase, the bacterial production (BP) was calculated. The difference between the BCD and BP is essentially the carbon used for bacterial respiration (BR). The Bacterial growth efficiency (BGE) is a measure of how much of the carbon assimilated, is allocated to BP, hence utilized for biomass synthesis. BGE is calculated from the increase in bacterial abundance converted to biomass production and the decrease in DOC concentration. The community growth rate (µ) was calculated as the ratio of BP to BB.

2.7. Respiration and production of specific bacterial populations

Samples (5 mL) for the enumeration of respiring cells were incubated with Bac Light Redox Sensor Green (RSG) Vitality Kit (ThermoFisher; 1 µM final concentration) for 30 min in the dark at room temperature. RSG is a fluorogenic reagent which becomes fluorescent after the interaction with a reductase enzyme (i.e., cellular respiration). After, the cells were fixed with formaldehyde (2% final concentration) in Cryo Tubes and stored at 4°C for 10 min and finally at –80°C.

Samples for production measurements (5 mL) were incubated with Click-iT homopropargylclycine (HPG) Alexa Fluor 488 Protein Synthesis Assay Kit

Kit (ThermoFisher; 20 nM final concentration) in the dark at room temperature for 4 h. HPG is a methionine analogue which is used for protein synthesis. Right after

incubation the cells were fixed with formaldehyde (2% final concentration) in Cryo Tubes and stored at 4°C for 10 min and finally at –80°C.

The abundance of respiring and producing bacteria was determined on a single cell level. After incubation, samples were filtered as described above (see Chapter 2.4 Estimating microbial cell abundance) and further processing according to Tinta *et al.* (2020). After filtration, RSG filters were treated according to the fluorescence in situ hybridization (FISH) protocol as explained below. To detect HPG incorporating bacteria, click chemistry was used, where the alkyne modified HPG is detected with Alexa Fluor 488 azide (Ex/EM = 490/525 nm). HPG filter pieces were placed into 200 µL of Click-iT® reaction buffer (154.5 µL Sigma water, 20 µL Click-iT reaction buffer, 20 µL 10x reaction buffer additive, 4 µL copper (II) sulfate, 1.6 µL Alexa Fluor 488 azide) and incubated in the dark at room temperature for 30 min, following the manufacturer's protocol. After the incubation, filter pieces were rinsed with MiliQ water (3x) and air-dried. Next, samples were treated according to the FISH protocol as described below.

2.8. Enumerating specific bacterial groups using fluorescence in situ hybridization (FISH)

The total abundance of bacteria and specific targeted bacterial groups was estimated by applying FISH. The oligonucleotide probes labelled with Cy3 and the 5'-end (Biomers) to target specific bacterial groups were chosen based on the the *A. aurita* degradation experiments of Tinta *et al.* (2020). The same probes were chosen as used earlier for the jellyfish degradation experiment (Tinta *et al.*, 2020) to compare degradation dynamics between different sources of GZ-OM as well as the same FISH protocol. To quantify all bacteria, a combination of probe EUB388 I, II and III was applied. To target specific bacterial populations, i.e., *Pseudoalteromonas, Alteromonas* and *Vibrio*, the probes PSU730, alter2 and GV, respectively, were used. **Error! Reference source not found.** shows the complete list of probes and their 5'-3' sequence including the respective references.

Both, HPG and RSG filters were mounted with a DAPI-mix after the FISH treatment, to determine the total abundance of respiring or biomass synthesizing cells by counting individual cells with overlying DAPI and RSG/HPG signals with the DAPI and FITC (Ex/EM = 495/519 nm) filter set, respectively. To determine the total abundance

of respiring/biomass synthesizing specific bacterial cells, individual cells were counted with overlying DAPI, RSG/HPG and FISH signals (see
for calculations of bacterial group activity). Cells were counted using a ZEISS AxioImager2 microscope equipped with specific filter sets for DAPI (Ex/Em = 358/461 nm), Cy3 fluorophore (Ex/Em = 554/568 nm) and FITC (Ex/Em = 495/519 nm) at 1,250x magnification. A minimum of 20 fields was counted for each filter slice using the software ACMEtool3.

Table 1 | FISH probes including references used to target specific bacterial genera. Abbreviations stand for the following groups: Eub = Bacteria, alter = Alteromonas, PSU = Pseudoalteromonas, GV = Vibrio.

Probe	**Specificity**	**Sequence 3‘- 5‘**	**Reference**
Eub338 I	Bacteria	GCT GCC TCC CGT AGG AGT	Amman *et al.* 1990
Eub338 II	Bacteria	GCA GCC ACC CGT AGG TGT	Daims *et al.* 1999
EUB338 III	Bacteria	GCT GCC ACC CGT AGG TGT	Daims *et al.* 1999
alter2	*Alteromonas*	GGT CCG CTC CAC ATC ACT GT	Demanèche *et al*. 2008
PSU730	*Pseudo-alteromonas*	TTG ACC CAG GTG GCT GCC	Huggett *et al.* 2008
GV	*Vibrio*	AGG CCA CAA CCT CCA AGT AG	Eilers *et al.* 2000

Table 2 | Calculations of total community cell abundance, total bacterial cell abundance, total active bacterial cells, and total active specific bacterial cells.

Groups	**Calculations using fluorescence signals**
Total Community	DAPI
Total Bacteria cells	DAPI + EUB I, II & III (FISH)
Total RSG/HPG positive (=active) bacterial cells	DAPI + EUB (FISH) + FITC
Specific bacterial cells	[DAPI + FISH (ALT|GV|PSU)] / Total bacteria
Specific RSG/HPG positive (=active) bacterial cells	[DAPI + FISH (ALT|GV|PSU) + FITC] / Total active bacteria

3. RESULTS

3.1. Microbial response to Cteno-OM amendment

During the course of the microcosm experiment microbial abundance was determined in the cteno-OM (J) as well as the control bottles (C). Initially, the microbial abundance was ~1 x 10^5 cells mL^{-1} in all bottles. The prokaryotic community showed a rapid response to the amendment with cteno-OM and reached an abundance of 7.2±1.2 x 10^6 mL^{-1} in the late exponential phase after 21 h (**Error! Reference source not found.**). The microbial abundance in the unamended control treatment did not exceed 0.8±0.1 x 10^6 cells mL^{-1}.

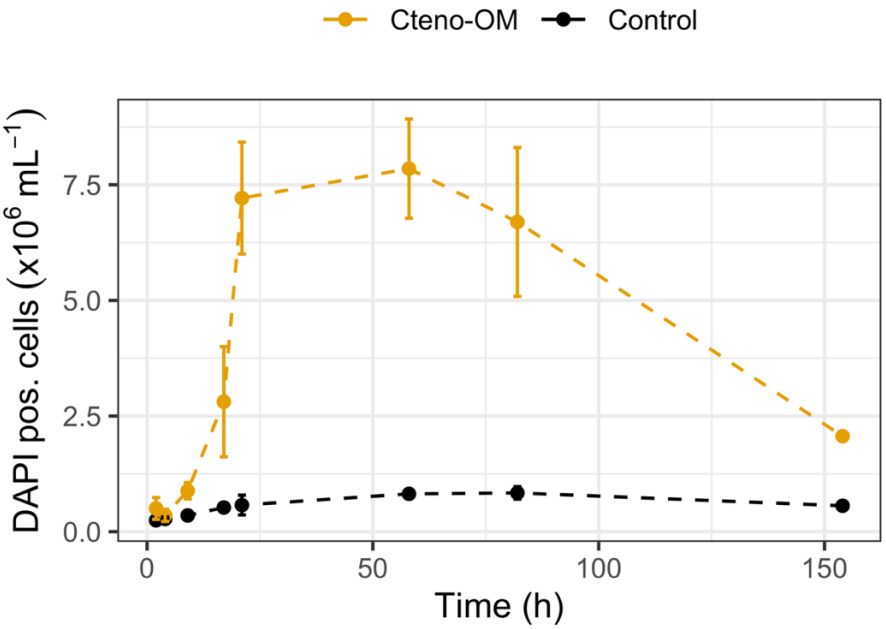

Figure 1 | Microbial abundance in the incubations with ctenophore organic matter (Cteno-OM) and in the unamended control treatment. Dots show averages of three biological replicates ± SD.

3.2. Dissolved organic carbon (DOC) release following cteno-OM amendment

The addition of 100 mg of cteno-OM L^{-1} to the incubation flasks led to an initial increase in DOC by ~21 µM DOC (Figure 2). The maximum DOC concentration was 184.5 µM measured after 17h (Figure 2). The individual bottles reached their maximum at different timepoints (J1 after 9 h, J2 after 17 h, J3 after 21 h), which we attribute to the heterogeneity of the sample. After 82 h, DOC within the cteno-OM bottles reached similar concentrations to the unamended control flasks (103.8 µM).

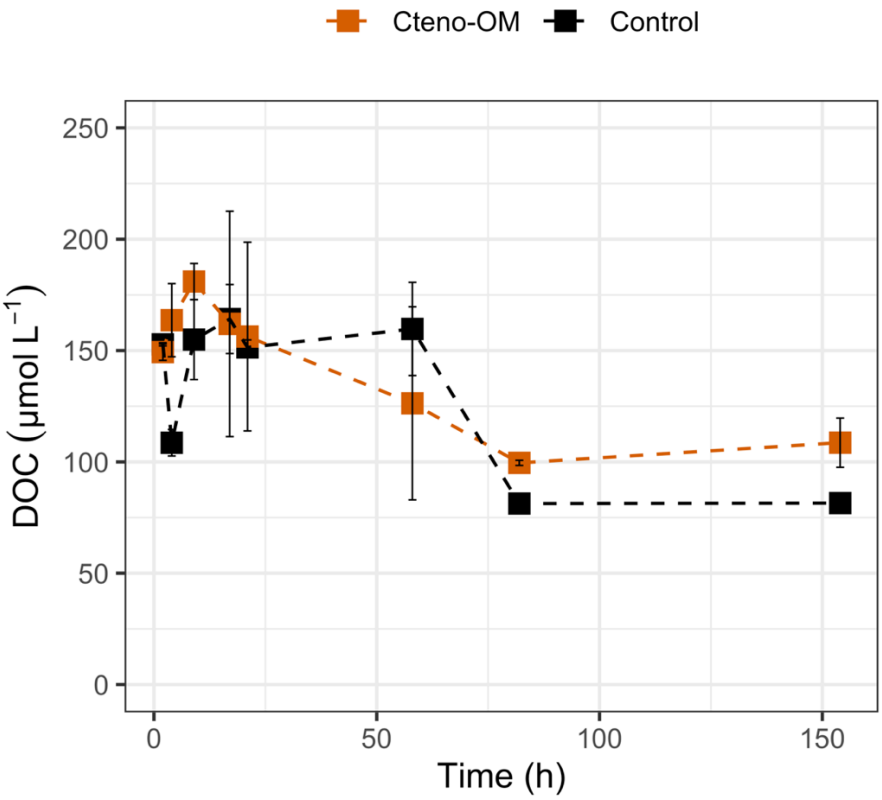

Figure 2 | Dissolved organic carbon (DOC) concentrations in the incubations amended with cteno-OM. Symbols represent averages ± SD of triplicate bottles

3.3. Microbial processing of ctenophore DOC

In the treatments amended with cteno-OM the DOC consumed during the exponential growth of heterotrophic bacteria resulted in a bacterial carbon demand (BCD) of 52.7±10 µg C L^{-1} h^{-1} (Table 3). The assimilated carbon was either respired by bacteria or incorporated into bacterial biomass. The increase in bacterial biomass (BB) during the exponential phase resulted in a BP of 11.7±11.2 µg C L^{-1} h^{-1} (Table 3). BR accounted for the rest of the DOC taken up by the bacterial community and amounted to 41±11.2 µg C L^{-1} h^{-1} (Table 3). This resulted in a bacterial growth efficiency (BGE) of 22.8±6.5% (Figure 3). The community growth rate during exponential growth was 0.07±0.003 h^{-1} (Table 3). In contrast, BGE in the unamended controls averaged 5% and exponential growth 0.04 (Table 3).

Table 3 | Bacterial community growth parameters based on DAPI counts expressed as averages of biological replicate bottles ± SD. Abbreviations stand for bacterial carbon demand (BCD), biomass

production at peak of abundance (BB), specific growth rate (μ), bacterial production (BP), bacterial respiration (BR) and bacterial growth efficiency (BGE). P-values derived from Student's t-test).

Growth parameters	Cteno-OM	Control
BCD (ΔDOC) (μg C L^{-1} h^{-1})	52.7±10	18.6
BB (μg C L^{-1})	144.2±24.2	11.5±4.3
μ (h^{-1})	0.07±0.003	0.04±0.02
BP (μg C L^{-1} h^{-1})	10.5±2.1	0.5±0.4
BR (μg C L^{-1} h^{-1})	41±11.2	17.7
BGE (%)	22.8±6.6	5

3.4. Respiration of specific bacterial groups

In the RSG incubation experiment, a total of 1.9±4.3 x 10^6 cells mL^{-1} (DAPI-positive) were counted in the late exponential phase (after 21 h) and 1.1±1.7 x 10^6 cells mL^{-1} at the collapse of the community (Figure 3) after 154 h in the cteno-OM enriched bottles. The cell abundance in the control bottles was half of that than in the cteno-OM treatment in the late exponential phase (0.9±0.4 x 10^6 cells mL^{-1}) and in the senescent phase (0.6 x 10^6 cells mL^{-1}).

In the bacterial inoculum 59% (0.7 x 10^6 cells mL^{-1}) of all cells (1.2 x 10^6 cells mL^{-1}) were actively respiring cells (DAPI + RSG positive). In the late exponential phase of the cteno-OM treatment 95±1% (1.8±0.4 x 10^6 cells mL^{-1}) of all cells were respiring (Figure 3). At the same timepoint, the control treatment exhibited less than half the cell abundance (0.8±0.5 x 10^6 cells mL^{-1}) with 83±1% respiring. At the end of the experiment, 133 h later, a large fraction of the total community (1.1±0.2 x 10^6 cells mL^{-1}) was still respiring (71±9%) while the absolute abundance decreased (0.8±0.2 x 10^6 cells mL^{-1}, Figure 3) in the cteno-OM treatment. In the control treatment, less than half of all the cells were identified as respiring cells (48%) and the total cell abundance was 0.3 x 10^6 cells mL^{-1} at the same timepoint.

In the cteno-OM treatment, 98±0.2% (1.7±0.4 x 10^6 cells mL^{-1}) were bacterial cells (DAPI + RSG + FISH-EUB positive) in the late exponential phase (Figure 3). At the end of the experiment the absolute abundance of respiring bacteria decreased to 0.8±0.2 x 10^6 cells mL^{-1} representing 92±1.5% of the total community (Figure 3).

The respiring community of the inoculum contributed 70.5% to the total bacterial abundance (Figure 3).The selected probes only targeted ~6.5% of the total bacterial community (DAPI + RSG + FISH positive, Figure 4). Of these 6.5% about 1.9% were respiring *Vibrio* cells, 2.9% were respiring *Alteromonas* cells and 2.5% were respiring *Pseudoalteromonas* cells. Within the cteno-OM treatment 29±6.3% of all respiring bacteria were *Pseudoalteromonas*, 4%±2.6 *Alteromonas* and 3.5%±3.1% *Vibrio* cells in the late exponential phase (Figure 4). These three targeted genera decreased in their contribution to the total bacterial abundance in the senescent phase (Figure 4). In the late exponential phase, the respiring bacterial community (0.8±0.4 x 10^6 cells mL^{-1}) in the control treatment contributed 81.6±4.8% to the total bacterial abundance. In the senescent phase, 72.6% of the 0.3 x 10^6 respiring cells mL^{-1} were identified as bacterial cells in the control treatment. The bacterial community was targeted to a minor extend with the specific probes at all timepoints in the control treatment (Figure 4). For technical reasons, two flasks of the control treatment were not available at the end of the experiment (T7). Details of the RSG-incubation experiment are given in Supplement 2.

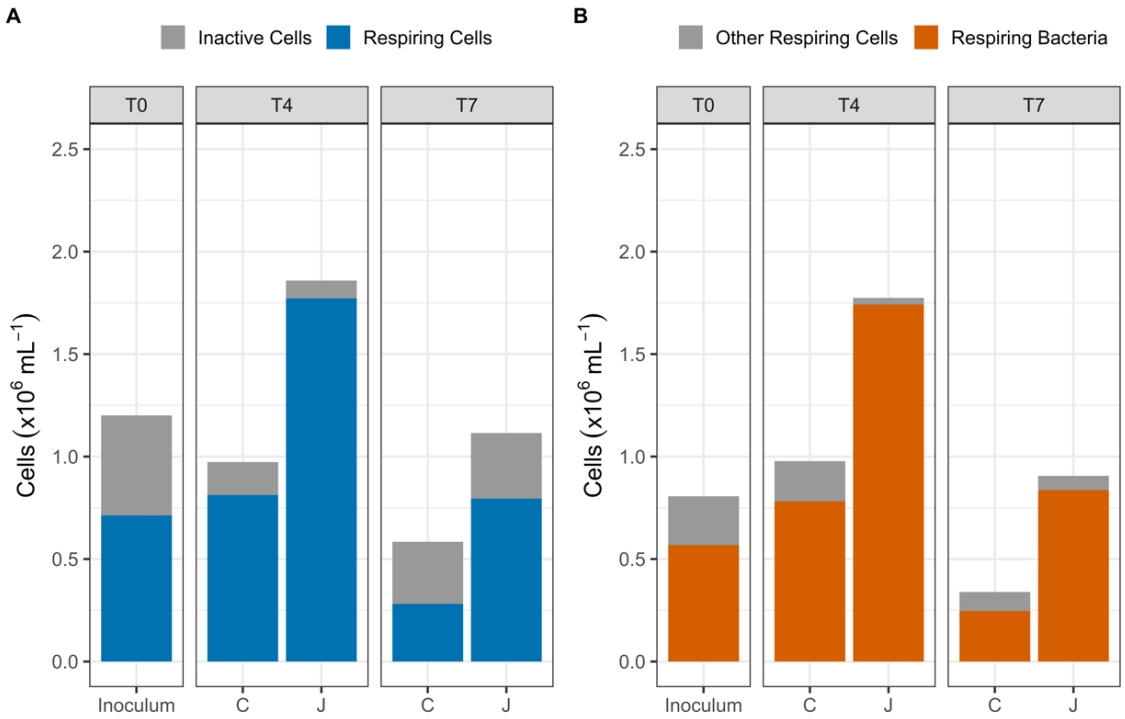

Figure 3 | A) Development of respiring microbial cells (blue) of all detected cells (entire column). Averages of three biological triplicate bottles are depicted. B) Respiring bacterial cells (orange) of all respiring cells detected (entire column). Standard deviations can be found in Supplementary 2. C =

control treatment, J = cteno-OM treatment. T0 = bacterial inoculum, T4 = late exponential phase of microbial growth and T7 = senescent phase of microbial growth.

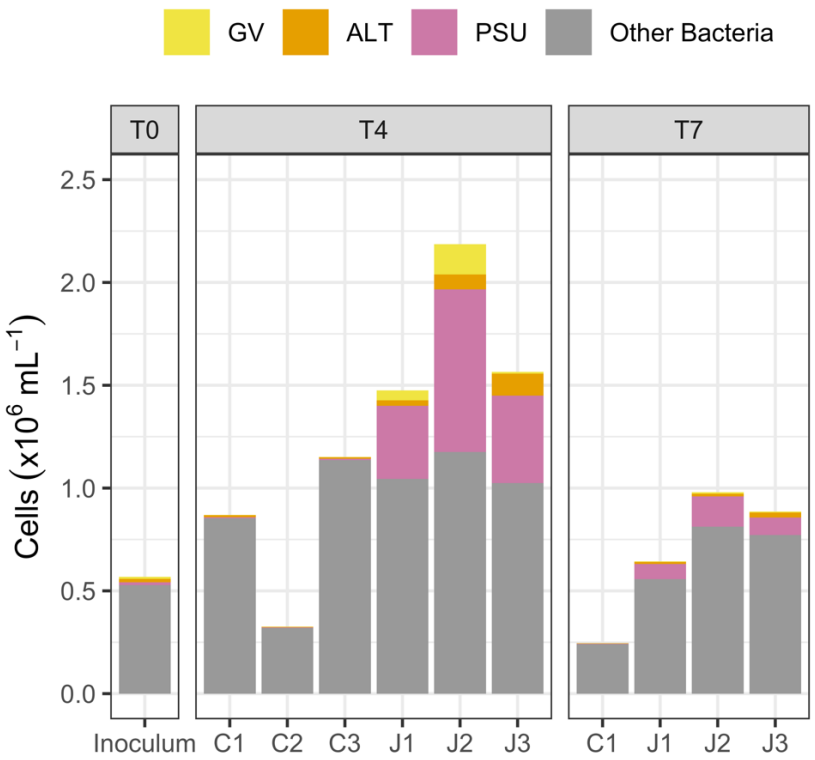

Figure 4 | Respiring targeted bacterial groups of all respiring bacteria. GV = Vibrio, ALT = Alteromonas, PSU = Pseudoalteromonas. Triplicate incubations are shown. C = control bottles, J = cteno-OM enriched bottles. T0 = bacterial inoculum, T4 = late exponential phase of microbial growth and T7 = senescent phase of microbial growth.

3.5. Biomass synthesis of specific bacterial groups

The incubation experiment with the methionine analogue HPG was linked to click-IT chemistry and the FISH method. A total of 7.9±5.2 x 10^6 cells mL^{-1} were counted in the late exponential phase (after 21 h) and 1.2±0.3 x 10^6 cells mL^{-1} at the collapse of the population (Figure 3) after 154 h in the cteno-OM amended treatment. In the control treatment, the abundance was substantially lower in the late exponential phase (1.5 ± 1.4 x 10^6 cells mL^{-1}) and at the collapse of the population (1.2±0.3 x 10^6 cells mL^{-1} than in the cteno-OM treatment (Figure 1). The cell abundance in the HPG-incubation was higher than in the RSG-incubation (**Error! Reference source not found.**).

In the bacterial inoculum 35% (0.6 x 10^6 cells mL^{-1}) of all targeted cells were metabolically active, i.e., incorporating HPG (DAPI + HPG positive, Figure 5). The

biomass synthesizing fraction of the cells in the cteno-OM treatment reached 55±2.8% of the total microbial abundance and remained high until the end of the experiment (Figure 5). Bacteria (DAPI + HPG + EUB) contributed 97.4±1.1% (4.2±3.1 x 10^6 cells mL^{-1}) and 77.9±5.5% to the biomass synthesizing community in the late exponential and senescent phase, respectively (Figure 5). In the control treatment, cells were similarly active in terms of HPG incorporation (66±12.2% in the late exponential phase, 60.3±5% in the senescent phase) as in the cteno-OM treatment. However, the absolute abundance of biomass synthesizing cells was much lower than in the cteno-OM treatment in the late exponential and senescent phase (Figure 5).

The biomass synthesizing community in the inoculum consisted to 41% of bacteria (Figure 5), while the selected probes only targeted 9% of them (DAPI + HPG + FISH positive, Figure 6). Of those about 4% were biomass synthesizing *Vibrio* cells, 4% *Alteromonas* and 1% *Pseudoalteromonas* cells. In the cteno-OM treatment, the oligonucleotide probes accounted for up to 68% of the biomass synthesizing bacterial community at the late exponential phase (Figure 6). *Pseudoalteromonas* contributed 50.3±27.6%, *Alteromonas* 9.5±5.2% and *Vibro* 9.3±8.8% to the entire HPG incorporating bacterial community (Figure 6). The abundance of biomass synthesizing bacteria decreased by the end of the experiment (after 154 h) to 40% of the HPG-positive bacteria (Figure 6).

In the late exponential phase, the respiring microbial community in the control treatment consisted to 70.7±18.5% of bacteria. In the senescent phase, 44% of the respiring cells were identified as bacterial cells. The bacterial community was targeted to a minor extend (<10%) with the specific probes at all timepoints (Figure 4). For the control treatment, flasks C2 and C3 were not available at the end of the experiment (T7) due to technical reasons. In the cteno-OM treatment, the J2 flask was excluded due to a three times lower cell abundance compared to the other cteno-OM flasks (**Error! Reference source not found.**). The complete list of averages and standard deviations of percentages and absolute cell abundances of the HPG-incubation is given in Supplement 3Supplement 3.

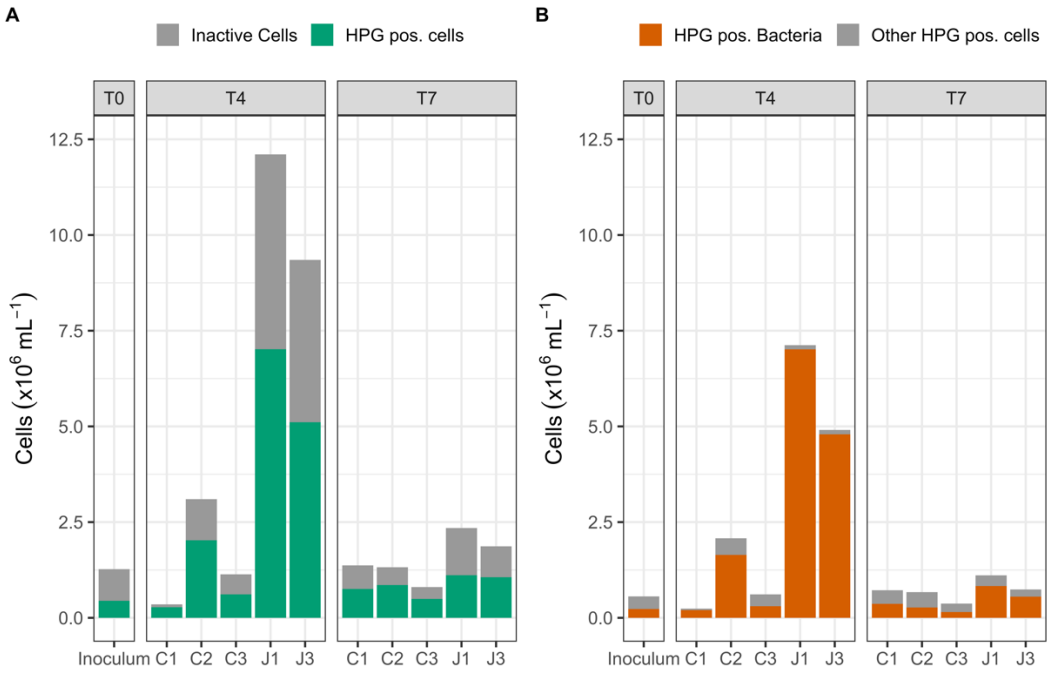

Figure 5 | A) HPG-positive cells (green) of all detected cells (entire column). Results depicted on a single bottle level to show heterogeneity between flasks. B) HPG-positive bacterial cells (orange) of all RSG-positive cells detected (entire column). Standard deviations can be found in Supplementary 3. C = control treatment, J = cteno-OM treatment. T0 = bacterial inoculum, T4 = late exponential phase of microbial growth and T7 = senescent phase of microbial growth.

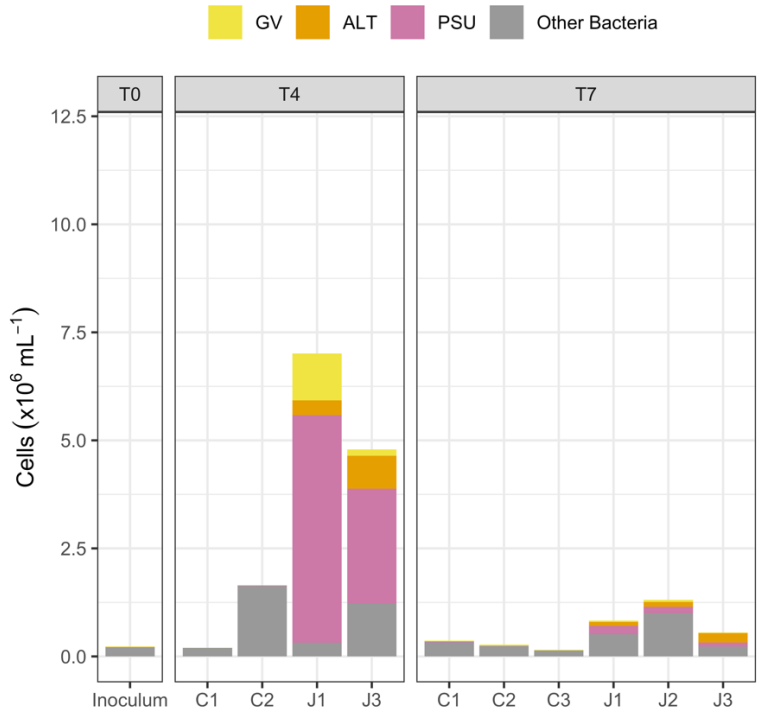

Figure 6 | HPG-positve targeted bacterial groups of all HPG-positive bacteria. GV = Vibrio, ALT = Alteromonas, PSU = Pseudoalteromonas. C = control treatment, J = cteno-OM treatment. T0 = bacterial inoculum, T4 = late exponential phase of microbial growth and T7 = senescent phase of microbial growth.

4. DISCUSSION

4.1. Processing of GZ-detritus

GZ populations are known for their boom-and-bust populations, followed by a major input of GZ-derived detrital matter input into the surrounding environment when GZ blooms are decaying. Thus, GZ can contribute substantially to local and regional detritus pools, especially in coastal and marine ecosystems (Lebrato *et al.*, 2012; Lucas *et al.*, 2014).

This thesis provides further insight into the microbial degradation of the widespread invasive species *M. leidyi*. The experimental design is similar to a previous study investigating the microbial processing of the cosmopolitan *Scyphozoa A. aurita* (Tinta *et al.*, 2020). The intention was to provide a better understanding of the differences and similarities between microbial degradation processes of gelatinous zooplankton species, characterized by differences in quantity and quality of OM comprising their biomass as well as different life histories.

We show that cteno-OM, like Jelly-OM (Tinta *et al.*, 2020), is rapidly utilized by a consortium of microorganisms, of which the large majority are bacteria (Figure 3, Figure 5). The addition of 100 mg L^{-1} ctenophore powder enriched the cteno-treatment with ~21 µM of DOC (**Error! Reference source not found.**). This is almost half of the amount released with the addition of 100 mg L^{-1} jellyfish powder as reported by Tinta *et al*. 2020 (~44 µM DOC). Bacteria processed the fresh cteno-DOC within 86 h, after which the DOC concentration reached similar concentrations to the control flasks and was similar to the DOC concentration of aged seawater (**Error! Reference source not found.**). While the dynamics of the DOC concentrations over time are comparable between the *A. aurita* study (Tinta *et al.*, 2020) and this study, the allocation of the assimilated carbon is different. The BCD of ctenophore degrading bacteria was twice as high (52.7 ± 10 µg C L^{-h} h^{-1},Table 3) as the BCD of the jellyfish degrading community (24.8 ± 16.1 µg C L^{-h} h^{-1}, Tinta *et al.*, 2020). Despite the utilization of twice the amount of DOC, bacterial biomass production based on cteno-OM was only half (Table 3) of the biomass production utilizing jellyfish-OM (Tinta *et al.* 2020). However, the specific growth rates were comparable (~1.8 d^{-1} in the ctenophore experiment, ~2 d^{-1} in the jellyfish experiment). Both, the jelly-OM and the cteno-OM amendment resulted in a higher growth rate than reported for the global ocean (0.1–1 d^{-1}, Ducklow, 1999; Kirchman, 2016). The BGE in the ctenophore treatment was 23% (Table 3)

indicating that the carbon taken up in the ctenophore treatment was mainly allocated to respiration rather than biomass production. This differs from the BGE of 65% obtained for jelly-OM (Tinta *et al.* 2020). Hence, ctenophore carbon is less likely to be incorporated into bacterial biomass and thus only to a smaller fraction of bacterial biomass is available to other consumers of the pelagic community than during jellyfish organic matter degradation. BGE of marine bacteria varies over a wide range depending on the nutrient status of the surrounding environment from 1% in oligotrophic systems and up to 60% in eutrophic systems (del Giorgio and Cole, 1998). Considering that the bacterial inoculum for this study was collected from a coastal oligotrophic system (northern Adriatic), the BGE of ctenophore degrading bacteria is still nevertheless fairly high.

4.2. Respiring and biomass synthesizing bacterial groups

The absolute DAPI-positive counts in the RSG-incubation were lower than the real time DAPI counts during the experiment (**Error! Reference source not found.**, Figure 3). We attribute this to two phenomena. First, looking at the frequency distribution of the real-time DAPI counts, we observed a few very high cell counts within the cteno-OM treatment, shifting the mean (Supplement 4, Supplement 5). These outliers are the result of a heterogenous distribution of microorganisms in the samples due to aggregate formation. Then, these aggregates existed in RSG-incubations as well but due to methodological limitations, such as the difficulty of counting aggregates with overlapping signals, these microscopy pictures were not included in the abundance calculation. This resulted in a lower overall cell abundance but a more homogenous distribution of counts between the individual fields of enumeration under the microscope.

The HPG-incubation resulted in higher absolute DAPI counts (in almost all bottles and at both timepoints) compared to the RSG-incubation as well as slightly higher DAPI counts as compared to the real-time DAPI counts (for almost all bottles except J bottles at T7) (Supplement 4, Supplement 5). This might be due to the fact that HPG-incubations were incubated for 4 h in cultivation flasks of a smaller volume, which means additional time available for cell growth with an amino acid analogue.

By targeting specific respiring/biomass synthesizing bacterial groups we aimed at better understanding the key players and the degradation process of different GZ

detritus in such a complex system like the coastal ocean. Respiring and biomass synthesizing communities in this experiment mainly consisted of bacterial cells (Figure 3, Figure 5). The same was recorded in the jellyfish experiment (Tinta *et al.*, 2020). *Pseudoalteromonas*, *Alteromonas* and *Vibro* are the main groups processing jellyfish detritus derived from *A. aurita*, comprising >90% of all biomass synthesizing and 55–95% of all respiring bacteria detected (Tinta *et al.*, 2020). In contrast to that, these three groups contributed substantially less to the bacterial consortium processing cteno-OM. Within the respiring community between 12–37% of respiring bacteria could be attributed to these three groups (Figure 4). In contrast, *Pseudoalteromonas*, *Alteromonas* and *Vibro* made up 31%–69% of the biomass synthesizing bacterial community during ctenophore degradation (Figure 6). In line with these finding is the preliminary taxonomic profile from metagenomic analysis of the microbial community degrading ctenophore detrital matter (Supplement 6). Compared to the fairly low bacterial diversity in the jellyfish organic matter degradation experiment (Tinta *et al.* 2020), the bacterial diversity in the ctenophore organic matter experiment was higher. The bacterial inoculums for the two experiments were taken during different months in autumn. The DOC concentration of the ambient seawater used for the ctenophore experiments was 103.8 µM while that for the jellyfish experiment was only ~80 µM (Tinta *et al*., 2020). This might indicate that the ambient seawater was characterized with DOM of different quantity and possibly quality potentially resulting in a different community composition of the inoculum.

Baas Becking postulated already in 1934, that concerning microbes “everything is everywhere, but the environment selects”. As ecological niches vanish and arise rapidly, so can microbial taxa potentially emerge from a microbial seedbank upon environmental triggers (Lennon and Jones, 2011; Welch and Huse, 2011). This implies that different sources of organic material can select for a different microbial community structure. Despite similarities in the biogeochemical body plan of GZ (ctenophore C:N 3.5±0.4, Supplement 7, jellyfish C:N 3.4±0.1, Lucas *et al.*, 2011; Tinta *et al.*, 2020), the derived detrital OM might not be all the same from a microbial point of view. In fact, one large difference potentially influencing microbial dynamics after the collapse of ctenophore blooms is the lack of nematocysts, as they are a unique feature of cnidarians. Apart from that, jellyfish and ctenophores do have very different life cycles with the former being holoplanktonic and reproducing asexually and most cnidarians being meroplanktonic as well as reproducing sexually. Furthermore, the

two groups of GZ do not occur during the same months in the northern Adriatic. *A. aurita* exhibits blooms from early spring to summer and *M. leidyi* blooms start in late summer and last through autumn (Kogovšek, Bogunović and Malej, 2010; Pestorić *et al.*, 2021).

Based on the analysis of FISH and the incubation experiments, we observed a structural change in the composition of the metabolically active bacterial community from the bacterial inoculum to the late exponential phase and then to the senescent phase (Figure 4, Figure 6) with only <15% of the respiring and biomass synthesizing community comprised of *Pseudoalteromonas*, *Alteromonas* and *Vibrio*. These observed shifts are in agreement with previous studies reporting an decrease of Alphaproteobacteria and an increase in Gammaproteobacteria growing on fresh and bioavailable jellyfish detritus (Tinta *et al.*, 2012, 2020; Dinasquet *et al.*, 2013; Blanchet *et al.*, 2015). At later stages of jelly-OM degradation, a succession of Bacteroidetes growing on more complex and presumably less-labile jellyfish-OM was observed (Tinta *et al.*, 2012, 2020; Dinasquet *et al.*, 2013; Blanchet *et al.*, 2015).

5. CONCLUSION

Taken together, this study shows that the decay of ctenophore blooms enriches the surrounding waters with DOC and triggers a rapid growth of bacterioplankton communities with specific growth rates higher than commonly reported for coastal marine ecosystems. Microbes degrading *M. leidyi* organic matter exhibit a lower BGE (~23%) than jellyfish degrading microbes. Three groups of opportunistic *Gammaproteobacteria (Pseudoalteromonas, Alteromonas, Vibrio*;) make up the majority of biomass synthesizing bacteria during the late exponential phase of microbial growth utilizing cteno-OM. This is in line with the composition of the bacterial consortium degrading jellyfish detritus. However, unlike in the degradation process of jellyfish detritus, there are other important key players involved in the utilization of *M. leidyi* detrital organic matter. We argue that detrital organic matter derived from decaying ctenophores can trigger different responses of the microbial community than DOM-derived from other GZ species. Overall, GZ blooms generate pulses of labile DOM with a C:N ratio of ~3.5 and hence, constitute a major perturbation for pelagic microbial communities, especially in oligotrophic marine systems like the northern Adriatic Sea.

6. ACKNOWLEDGEMENT

With this being an essential step of the beginning of my scientific career, I want to thank the people who have helped me come so far. An important person that I can probably not thank enough was and is Gerhard J. Herndl. He supported me in every possible way from my Bachelor of Science curriculum until now. Thank you, Gerhard, for all the efforts made, knowledge shared, advice and guidance given, and the constant support provided.

My deepest appreciation and gratefulness also go to Tinkara Tinta, who included me in her project and guided me through my Master's Thesis. She has introduced me to so many laboratory methods and is my role model when it comes to meticulous and efficient scientific work. Thank you, Tinkara, for your endless support, explanations, patience, and precise and constructive criticism through which I was constantly able to improve and grow. I feel incredible lucky, that you were my MSc. thesis co-supervisor and could not have imagine a better, more suitable mentor for myself.

Furthermore, I would like to thank Chie Amano who was happy to answer any question at any time and providing me with her expertise as well as Eddie Fadeev for his support not just during my struggling times with R. Another truthful thank you goes to Barbara Mähnert, our lab manager, who is always helping wherever she can. Lastly, I am grateful to the entire Microbial Oceanography unit - it was a pleasure to be part of it. While not contributing directly to my scientific work, I still consider it essential to thank Lisa Steurer and Robin Ströhle, who have been keeping me sane and providing me with a strong family network during my journey.

7. ZUSAMMENFASSUNG

In den letzten Jahrzehnten ist die *Ctenophora Mnemiopsis leidyi* in viele marine Ökosysteme eingedrungen und hat oft drastische Veränderungen in pelagischen Lebensgemeinschaften herbeigeführt. Als blütenbildendes gallertartiges Zooplankton kann die Ctenophore hohe Populationszahlen erreichen und potenziell wesentlich zum gelösten organischen Substanzenpool sowie anorganischen Nährstoffpool beitragen. Der Zerfall von *M. leidyi*-Kadavern, könnte heterotrophen Mikroben im umgebenden Wasser ein organisches Substrat bieten. In dieser Arbeit wurden die mikrobiellen Wachstumsparameter errechnet und die Konzentrationen des gelösten organischen Kohlenstoffs (DOC) gemessen, um mikrobielle Dynamiken nach dem Zusammenbruch des Ctenophor-Blooms und dessen Auswirkungen auf die Ökologie von Küstengewässern zu verfolgen. Wir zeigen, dass ein Zerfall einer typischen Ctenophor-Blüte, wenn etwa 100 mg Ctenophor Detritus Pulver (Cteno-OM) pro Liter verfügbar werden, das System mit ~ 21 µM DOC (oder 0,07 ± 0,01 µmol pro mg Cteno-OM) und löst ein schnelles mikrobielles Wachstum aus (µ = ~ 1,8 d-1). Kohlenstoff, der aus cteno-OM gewonnen wird, treibt eher die mikrobielle Atmung als die Biomasseproduktion an (bakterielle Wachstumseffizienz ~ 22%). *Pseudoalteromonas*, *Alteromonas* und *Vibrio* machen zusammen bis zu ~ 37 % aller atmenden Bakterienzellen und bis zu ~ 69 % der Biomasse produzierenden Bakteriengemeinschaft aus. Tinta *et al*. (2020) untersuchten den Abbau von *Aurelia aurita* mit einem identischen Versuchsaufbau. Vergleicht man unsere Ergebnisse mit der Studie von Tinta *et al.* (2020), wird daraus ersichtlich, dass unterschiedliche Quellen von gallertartigem organischem Zooplankton unterschiedliche mikrobielle und umweltbezogene Feedbacks hervorrufen.

8. REFERENCES

Anninsky, B. E. *et al.* (2005) 'Effect of starvation on the biochemical compositions and respiration rates of ctenophores Mnemiopsis leidyi and Beroe ovata in the Black Sea', *Journal of the Marine Biological Association of the United Kingdom*. 2005/06/21. Cambridge University Press, 85(3), pp. 549–561. doi: DOI: 10.1017/S0025315405011471.

Azam, F. and Malfatti, F. (2007) 'Microbial structuring of marine ecosystems', *Nature Reviews Microbiology*, 5(10), pp. 782–791. doi: 10.1038/nrmicro1747.

Bayer, B. *et al.* (2019) 'Ammonia-oxidizing archaea release a suite of organic compounds potentially fueling prokaryotic heterotrophy in the ocean', *Environmental Microbiology*. John Wiley & Sons, Ltd, 21(11), pp. 4062–4075. doi: 10.1111/1462-2920.14755.

Billett, D. S. M. *et al.* (2006) 'Mass deposition of jellyfish in the deep Arabian Sea', *Limnology and Oceanography*. John Wiley & Sons, Ltd, 51(5), pp. 2077–2083. doi: https://doi.org/10.4319/lo.2006.51.5.2077.

Blanchet, M. *et al.* (2015a) 'Changes in bacterial community metabolism and composition during the degradation of dissolved organic matter from the jellyfish Aurelia aurita in a Mediterranean coastal lagoon', *Environmental Science and Pollution Research*, 22(18), pp. 13638–13653. doi: 10.1007/s11356-014-3848-x.

Blanchet, M. *et al.* (2015b) 'Changes in bacterial community metabolism and composition during the degradation of dissolved organic matter from the jellyfish Aurelia aurita in a Mediterranean coastal lagoon', *Environmental Science and Pollution Research*, 22(18), pp. 13638–13653. doi: 10.1007/s11356-014-3848-x.

Carlson, C. A. and Hansell, D. A. (2015) 'Chapter 3 - DOM Sources, Sinks, Reactivity, and Budgets', in Hansell, D. A. and Carlson, C. A. B. T.-B. of M. D. O. M. (Second E. (eds). Boston: Academic Press, pp. 65–126. doi: https://doi.org/10.1016/B978-0-12-405940-5.00003-0.

Chelsky, A., Pitt, K. A. and Welsh, D. T. (2015) 'Biogeochemical implications of decomposing jellyfish blooms in a changing climate', *Estuarine, Coastal and Shelf Science*. Elsevier Ltd, 154, pp. 77–83. doi: 10.1016/j.ecss.2014.12.022.

Condon, R. H. *et al.* (2011) 'Jellyfish blooms result in a major microbial respiratory sink of carbon in marine systems', *Proceedings of the National Academy of Sciences of the United States of America*, 108(25), pp. 10225–10230. doi: 10.1073/pnas.1015782108.

Condon, R. H. *et al.* (2013) 'Recurrent jellyfish blooms are a consequence of global oscillations', *Proceedings of the National Academy of Sciences of the United States of America*, 110(3), pp. 1000–1005. doi: 10.1073/pnas.1210920110.

Costello, J. H. *et al.* (2012) 'Transitions of Mnemiopsis leidyi (Ctenophora: Lobata) from a native to an exotic species: a review', *Hydrobiologia*, 690(1), pp. 21–46. doi: 10.1007/s10750-012-1037-9.

Dinasquet, J. *et al.* (2013) 'Functional and compositional succession of bacterioplankton in response to a gradient in bioavailable dissolved organic carbon', *Environmental Microbiology*, 15(9), pp. 2616–2628. doi: 10.1111/1462-2920.12178.

Dinasquet, J., Granhag, L. and Riemann, L. (2012) 'Stimulated bacterioplankton growth and selection for certain bacterial taxa in the vicinity of the ctenophore Mnemiopsis leidyi', *Frontiers in Microbiology*, 3(AUG), pp. 1–8. doi: 10.3389/fmicb.2012.00302.

Ducklow, H. W. (1999) 'The bacterial component of the oceanic euphotic zone', *FEMS Microbiology Ecology*, 30(1), pp. 1–10. doi: 10.1111/j.1574-6941.1999.tb00630.x.

Dunlop, K. M., Jones, D. O. B. and Sweetman, A. K. (2017) 'Direct evidence of an efficient energy transfer pathway from jellyfish carcasses to a commercially important deep-water species', *Scientific Reports*, 7(1), p. 17455. doi: 10.1038/s41598-017-17557-x.

Field, C. B. *et al.* (1998) 'Primary production of the biosphere: Integrating terrestrial and oceanic components', *Science*, 281(5374), pp. 237–240. doi: 10.1126/science.281.5374.237.

del Giorgio, P. A. and Cole, J. J. (1998) 'Bacterial growth efficiency in natural aquatic systems', *Annual Review of Ecology and Systematics*. Annual Reviews, 29(1), pp. 503–541. doi: 10.1146/annurev.ecolsys.29.1.503.

Hansell, D. A. *et al.* (no date) 'Dissolved organic matter in the ocean a controversy stim ulates new insights', *Oceanography*, 22(SPL.ISS. 4), pp. 202–211. doi: 10.5670/oceanog.2009.109.

Hansell, D. A., Williams, P. M. and Ward, B. B. (1993) 'Measurements of DOC and DON in the Southern California Bight using oxidation by high temperature combustion', *Deep-Sea Research Part I*, 40(2), pp. 219–234. doi: 10.1016/0967-0637(93)90001-J.

Hansson, L. (1997) 'Effect of temperature on growth rate of Aurelia aurita (Cnidaria, Scyphozoa) from Gullmarsfjorden, Sweden', *Marine Ecology Progress Series*, 161, pp. 145–153.

Hoegh-Guldberg, O., R. Cai, E.S. Poloczanska, P.G. Brewer, S. Sundby, K. Hilmi, V.J. Fabry, and S. J. (2014) *IPCC, 2014: Climate Change 2014: Adaptation, and Vulnerability. Contribution of Working Group II to the Fifth Assessment Report of the Intergovernmental Panel on Climate Change*, *Cambridge University Press, Cambridge, United Kingdom and New York, NY, USA*.

Jaspers, C. *et al.* (2018) 'Ocean current connectivity propelling the secondary spread of a marine invasive comb jelly across western Eurasia', *Global Ecology and Biogeography*, 27(7), pp. 814–827. doi: 10.1111/geb.12742.

Kirchman, D. L. (2016) 'Growth Rates of Microbes in the Oceans', *Annual Review of Marine Science*. Annual Reviews, 8(1), pp. 285–309. doi: 10.1146/annurev-marine-122414-033938.

Kogovšek, T. *et al.* (2014) 'Jellyfish biochemical composition: Importance of standardised sample processing', *Marine Ecology Progress Series*, 510, pp. 275–288. doi: 10.3354/meps10959.

Kogovšek, T., Bogunović, B. and Malej, A. (2010) 'Recurrence of bloom-forming scyphomedusae: Wavelet analysis of a 200-year time series', *Hydrobiologia*, 645(1), pp. 81–96. doi: 10.1007/s10750-010-0217-8.

Lebrato, M. *et al.* (2012) 'Jelly-falls historic and recent observations: A review to drive future research directions', *Hydrobiologia*, 690(1), pp. 227–245. doi: 10.1007/s10750-012-1046-8.

Lebrato, M. *et al.* (2019) 'Sinking of Gelatinous Zooplankton Biomass Increases Deep Carbon Transfer Efficiency Globally', *Global Biogeochemical Cycles*, 33(12), pp. 1764–1783. doi: 10.1029/2019GB006265.

Lee, S. and Fuhrman, J. A. (1987) 'Relationships between Biovolume and Biomass of Naturally Derived Marine Bacterioplankton', *Applied and environmental microbiology*, 53(6), pp. 1298–1303. doi: 10.1128/aem.53.6.1298-1303.1987.

Lennon, J. and Jones, S. (2011) 'Microbial seed banks: The ecological and evolutionary implications of dormancy', *Nature reviews. Microbiology*, 9, pp. 119–130. doi: 10.1038/nrmicro2504.

Lucas, C. H. *et al.* (2011) 'What's in a jellyfish? Proximate and elemental composition and biometric relationships for use in biogeochemical studies', *Ecology*. John Wiley

& Sons, Ltd, 92(8), p. 1704. doi: https://doi.org/10.1890/11-0302.1.
Lucas, C. H. *et al.* (2014) 'Gelatinous zooplankton biomass in the global oceans: Geographic variation and environmental drivers', *Global Ecology and Biogeography*, 23(7), pp. 701–714. doi: 10.1111/geb.12169.
Luo, J. Y. *et al.* (2020) 'Gelatinous Zooplankton-Mediated Carbon Flows in the Global Oceans: A Data-Driven Modeling Study', *Global Biogeochemical Cycles*, 34(9). doi: 10.1029/2020GB006704.
Malej, A. *et al.* (2017) 'Mnemiopsis leidyi in the northern Adriatic: here to stay?', *Journal of Sea Research*, 124(July 2018), pp. 10–16. doi: 10.1016/j.seares.2017.04.010.
McNamara, M. E., Lonsdale, D. J. and Aller, R. C. (2013) 'Elemental Composition of Mnemiopsis leidyi A. Agassiz 1865 and Its Implications for Nutrient Recycling in a Long Island Estuary', *Estuaries and Coasts*, 36(6), pp. 1253–1264. doi: 10.1007/s12237-013-9636-x.
Molina-Ramírez, A. *et al.* (2015) 'Functional differences in the allometry of the water, carbon and nitrogen content of gelatinous organisms', *Journal of Plankton Research*, 37(5), pp. 989–1000. doi: 10.1093/plankt/fbv037.
Pestorić, B. *et al.* (2021) 'Scyphomedusae and ctenophora of the eastern adriatic: Historical overview and new data', *Diversity*, 13(5). doi: 10.3390/d13050186.
Pitt, K. A. *et al.* (2014) *Boom and bust: Why do blooms of jellyfish collapse?*, *Jellyfish blooms*. Edited by K. A. P. and C. H. Lucas. Springer.
Pitt, K. A. and Lucas, C. H. (2014) 'Jellyfish blooms', in *Jellyfish Blooms*, pp. 1–304. doi: 10.1007/978-94-007-7015-7.
Pitt, K. A., Welsh, D. T. and Condon, R. H. (2009) 'Influence of jellyfish blooms on carbon, nitrogen and phosphorus cycling and plankton production', *Hydrobiologia*, 616(1), pp. 133–149. doi: 10.1007/s10750-008-9584-9.
Purcell, J. E. (2011) 'Jellyfish and Ctenophore Blooms Coincide with Human Proliferations and Environmental Perturbations', *Annual Review of Marine Science*. Annual Reviews, 4(1), pp. 209–235. doi: 10.1146/annurev-marine-120709-142751.
Richardson, A. J. *et al.* (2009) 'The jellyfish joyride: causes, consequences and management responses to a more gelatinous future', *Trends in Ecology and Evolution*, 24(6), pp. 312–322. doi: 10.1016/j.tree.2009.01.010.
Shiganova, T. A. (1998) 'Invasion of the Black Sea by the ctenophore Mnemiopsis leidyi and recent changes in pelagic community structure', *Fisheries Oceanography*. John Wiley & Sons, Ltd, 7(3-4), pp. 305–310. doi: 10.1046/j.1365-2419.1998.00080.x.
Steinberg, D. K. and Landry, M. R. (2017) 'Zooplankton and the Ocean Carbon Cycle', *Annual Review of Marine Science*, 9(1), pp. 413–444. doi: 10.1146/annurev-marine-010814-015924.
Sweetman, A. K. *et al.* (2014) 'Rapid scavenging of jellyfish carcasses reveals the importance of gelatinous material to deep-sea food webs', *Proceedings of the Royal Society B: Biological Sciences*. Royal Society, 281(1796), p. 20142210. doi: 10.1098/rspb.2014.2210.
Sweetman, A. K. *et al.* (2016) 'Jellyfish decomposition at the seafloor rapidly alters biogeochemical cycling and carbon flow through benthic food-webs', *Limnology and Oceanography*, 61(4), pp. 1449–1461. doi: 10.1002/lno.10310.
Tinta, T. *et al.* (2010) 'Degradation of the Adriatic medusa Aurelia sp. by ambient bacteria', *Hydrobiologia*, 645(1), pp. 179–191. doi: 10.1007/s10750-010-0223-x.
Tinta, T. *et al.* (2012) 'Jellyfish Modulate Bacterial Dynamic and Community Structure', *PLOS ONE*. Public Library of Science, 7(6), p. e39274. Available at: https://doi.org/10.1371/journal.pone.0039274.

Tinta, T. *et al.* (2016) 'Microbial transformation of jellyfish organic matter affects the nitrogen cycle in the marine water column - A Black Sea case study', *Journal of Experimental Marine Biology and Ecology*, 475, pp. 19–30. doi: 10.1016/j.jembe.2015.10.018.

Tinta, T. *et al.* (2020) 'Microbial Processing of Jellyfish Detritus in the Ocean', *Frontiers in Microbiology*, 11(October), pp. 1–18. doi: 10.3389/fmicb.2020.590995.

Tinta, T., Klun, K. and Herndl, G. J. (2021) 'The importance of jellyfish–microbe interactions for biogeochemical cycles in the ocean', *Limnology and Oceanography*, 66(5), pp. 2011–2032. doi: 10.1002/lno.11741.

Tiselius, P. and Møller, L. F. (2017) 'Community cascades in a marine pelagic food web controlled by the non-visual apex predator Mnemiopsis leidyi', *Journal of Plankton Research*, 39(2), pp. 271–279. doi: 10.1093/plankt/fbw096.

Titelman, J. *et al.* (2006) 'Turnover of dead jellyfish: Stimulation and retardation of microbial activity', *Marine Ecology Progress Series*, 325, pp. 43–58. doi: 10.3354/meps325043.

Vinogradov, M.E., Shushkina, E.A., Musaeva, E.I., Sorokin, P. Y. (1989) 'Ctenophore Mnemiopsis leidyi (A. Agassiz) (Ctenophora: Lobata) - new settlers in the Black Sea.', *Oceanology*, (29), pp. 293–298.

Welch, D. B. M. and Huse, S. M. (2011) 'Microbial Diversity in the Deep Sea and the Underexplored "Rare Biosphere"', *Handbook of Molecular Microbial Ecology II: Metagenomics in Different Habitats*, (30), pp. 243–252. doi: 10.1002/9781118010549.ch24.

West, E. J. *et al.* (2009) 'Top-down and bottom-up influences of jellyfish on primary productivity and planktonic assemblages', *Water*, 54(6), pp. 2058–2071. doi: 10.4319/lo.2009.54.6.2058.

West, E. J., Welsh, D. T. and Pitt, K. A. (2009) 'Influence of decomposing jellyfish on the sediment oxygen demand and nutrient dynamics', *Hydrobiologia*. Dordrecht: Springer Nature B.V., 616(1), pp. 151–160. doi: http://dx.doi.org/10.1007/s10750-008-9586-7.

Wright, R. M. *et al.* (2020) 'Unique role of jellyfish in the plankton ecosystem revealed using a global ocean biogeochemical model', *Biogeosciences Discussions*, pp. 1–43. doi: 10.5194/bg-2020-136.

9. APENDIX

Supplement 1 | The dry mass in gram of each of the 21 M. leidyi individuals sampled.

m_1= 4.342g	m_{12}= 0.847g
m_2= 4.202g	m_{13}= 0.702g
m_4= 0.932g	m_{14}= 0.747g
m_5=1.497g	m_{16}= 1.022g
m_6= 1.327g	m_{17}= 0.637g
m_7= 1.202g	m_{18}= 0.787g
m_8=1.447g	m_{19}= 0.707g
m_9= 1207g	m_{20}= 0.597g
m_{10}= 1.382g	m_{21}= 0.532g
m_{11}= 1.362g	

Supplement 2 | List with absolute and percentage values of the RSG-incubation.

	T0	**Late exponential (T4)**		**Senescent (T7)**	
	Inoculum	**Cteno-OM**	**Control**	**Cteno-OM**	**Control**
Total cells (10^5 cells mL^{-1})	12.0	18.6±4.3	9.7±4.4	11.1±1.7	5.8
Respiring cells (%)	59%	95±1	83±1	71±9	48
Total respiring cells (10^5 cells mL^{-1})	7.1	17.7±4.1	8.1±3.7	8±2	2.8
% Respiring Bacteria	70.5	98.2±0.2	81.6±4.8	92.1±1.5	72.6
Respiring Bacterial Abund. (10^5 cells/mL)	5.7	17.4±3.9	7.8±4.2	8.4±1.7	2.4
% of respiring GV	1.9	3.5±3.1	0.2±0.2	0.6±0.2	0.7
% of respiring ALT	2.9	4.0±2.6	0.8±0.2	1.9±0.7	0.2
% of respiring PSU	2.5	29.1±6.3	0.6±0.1	12.1±2.7	1.2

Supplement 3 | List with absolute and percentage values of HPG-incubation.

	T0	**Late exponential (T4)**		**Senescent (T7)**	
	Inoculum	**Cteno-OM**	**Control**	**Cteno-OM**	**Control**

Total cells (10^5 cells mL^{-1})	12.7	78.6±51.6	15.3±14.2	25.1±7.5	11.6±3.1
HPG-positive cells (%)	34.9	55±2.8	66±12.2	51±5	60.3±5
Total HPG-positive cells (10^5 cell/mL)	5.6	43±31.8	9.8±9.7	11.4±4.1	5.9±1.9
% HPG-positive Bacteria	41	97.4±1.1	70.7±18.5	77.9±5.5	44
HPG-positive Bacterial Abundance (10^5 cells/mL)	2.3	42.1±31.4	7.2±8.1	9±3.8	2.6±1.1
% of HPG-positive GV	4	9.3±8.8	0.4±0.3	3.5±0.5	7.2±2.8
% of HPG-positive ALT	4	9.5±5.7	0.4±0.2	19.5±17.1	1.2±0.6
% of HPG-positive PSU	1	50.3±27.6	0.3±0.4	17.4±5.9	1.8±2.7

Supplement 4 | Frequency distribution of DAPI-positive cell counts at the late exponential phase (T4) of heterotrophic growth in the Cteno-OM treatment (J1–J3) and the control treatment (C1–C3). X-axis depicts the frequency of the count bins, y-axis shows cell mL^{-1}. Cell counts from the HPG-incubation experiment in red, the microscopy direct real-time counts in green, and in blue the RSG-incubation cell counts. The abbreviations above the bottle ID's stand for the probes used on that filter piece. However, for these counts only the DAPI signal was considered. The dotted straight lines represent the mean of the fields of views (FOV's) and the straight line represents the median of the FOV's.

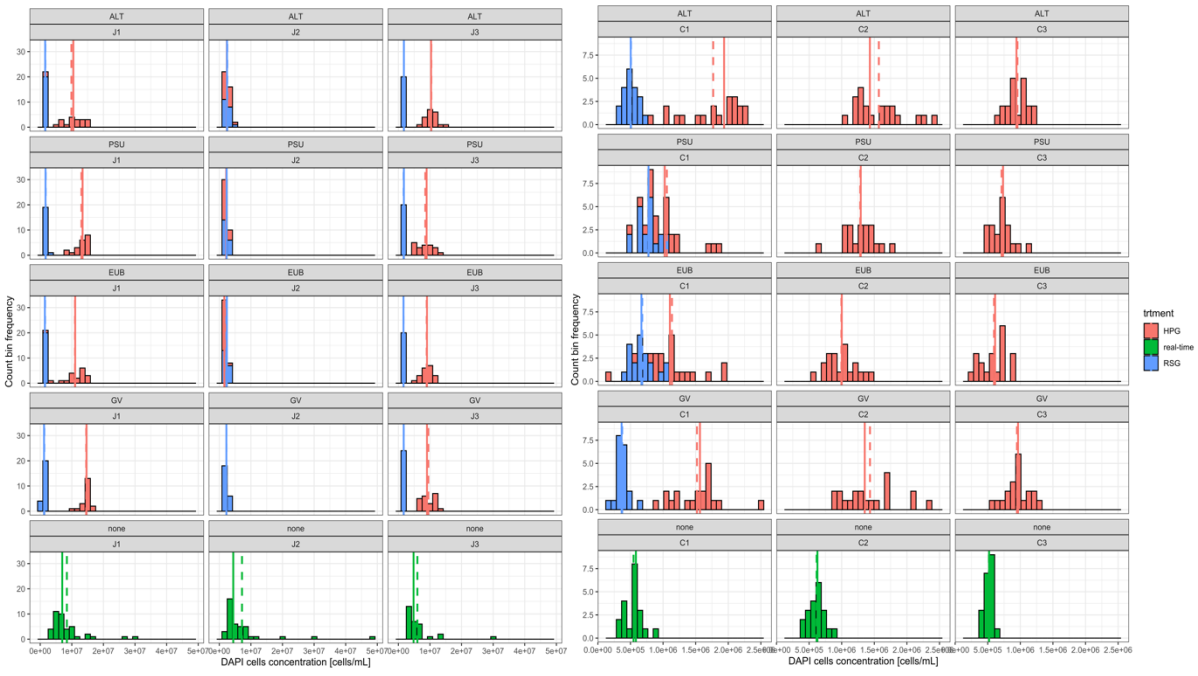

Supplement 5 | Frequency distribution of DAPI-positive cell counts at the senescent phase (T7) of heterotrophic growth in the Cteno-OM treatment (J1–J3) and the control treatment (C1–C3). X-axis depicts the frequency of the count bins, y-axis shows cell mL-1. Counts from the HPG-incubation experiment in red, the microscopy direct real-time counts in green, and in blue the RSG-incubation cell counts. The abbreviations above the bottle ID's stand for the probes used on that filter piece. However, for these counts only the DAPI signal was considered. The dotted straight lines represent the mean of the fields of views (FOV's) and the straight line represents the median of the FOV's.

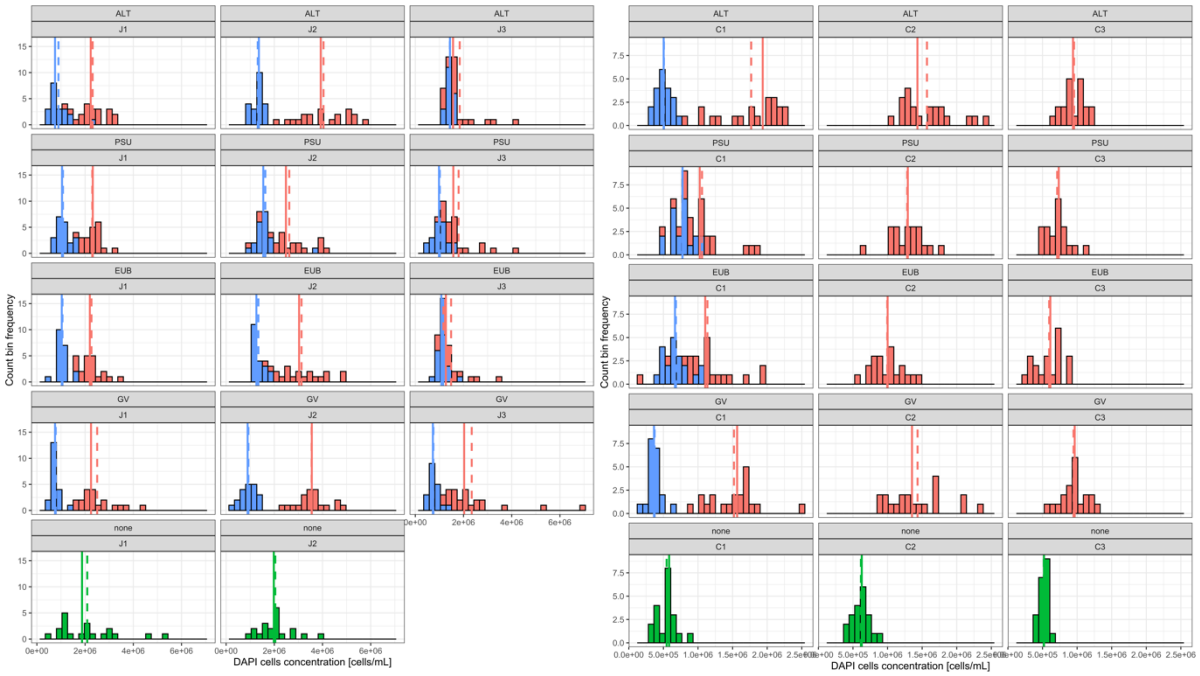

Supplement 6 | Preliminary metagenomic analysis. Taxonomic profiling of microbial metagenomes from the late exponential phase of the experiment.

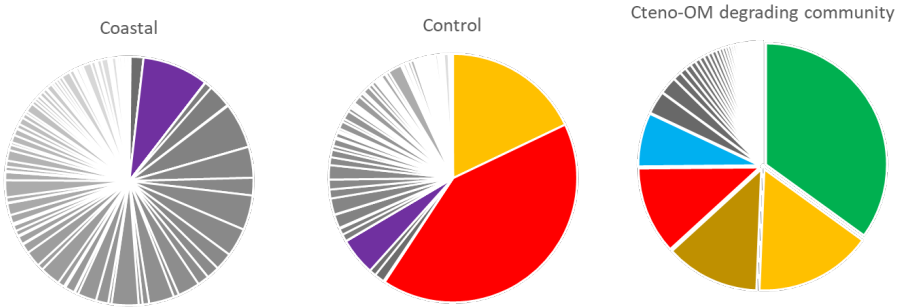

Pseudoalteromonas (**Bin 36**) ~ 35%, Pseudomonadales, Saccharospirillaceae (**Bin 45**) ~ 16% (in Control 18%), Pseudomonadales, Nitrincolaceae (**Bin 2**) ~ 13%, Alteromonas (**Bin 35**) ~ 12% (in Control 41%), Vibrio (**Bin 96**) ~ 7 %, Pseudomonadales, Halieaceae (**Bin 63**) ~ 9% in Coastal community, 5% in Control

Supplement 7 | Dissolved organic carbon (DOC) and total dissolved nitrogen (TDN) and C:N ratio of the leaching experiment in artificial sea water. Cteno-DM – ctenophore dry matter

	µmol per mg of cteno-DM
DOC	0.227 (±0.001)
TDN	0.7 (±0.01)
C:N	3.5 (±0.4)

Methodical description of bacterial DNA extraction and metagenomic analysis

For bacterial community structure analysis, we followed total nucleic acid extraction according to Angel *et al.* (2012) with some modifications for extracting from filters (Bayer *et al.*, 2019). To extract from filters, the tubes containing the filters were submerged in liquid nitrogen. Once the filters were completely frozen, they were fragmented into small pieces with a metal spatula (sterilized with 96% ethanol and burning). From then onwards, the extraction, purification and precipitation steps were following the procedure described by Angel *et al*. (2012). The quantification of metagenomic DNA, was done using the PicoGreen® dsDNA quantitation assay (ThermoFisher). The manufacturer's instructions were followed using the Infinite® 200 PRO (TECAN) plate reader with a transparent 96-well well plate to measure absorbance.

All metagenomic DNA libraries were constructed (Westburg kit, enzymatic shearing) and 125 bp paired-end sequenced on one lane of a HiSeqV4 Illumina platform at the Vienna Biocenter Core Facilities. Preliminary metagenomic analysis was done by Zihao Zhao from the Microbial Oceanography Unit at the University of Vienna.